ELSEVIER

Global and Planetary Change 29 (2001) 57–76

GLOBAL AND PLANETARY CHANGE

www.elsevier.com/locate/gloplacha

Modeling orbital forcing of lake level change: Lake Gosiute (Eocene), North America

Carrie Morrill [a,*], Eric E. Small [b], Lisa C. Sloan [a]

[a] *Department of Earth Sciences, University of California, Santa Cruz, Santa Cruz, CA 95064, USA*
[b] *Department of Earth and Environmental Science, New Mexico Institute of Mining and Technology, Socorro, NM 87801, USA*

Abstract

The sedimentary record of Lake Gosiute, a lake that existed in southwestern Wyoming during the Eocene, contains evidence for lake level fluctuations thought to be caused by the earth's precession cycle. However, it is not clear how the effects of these orbital variations were transferred through the climate system and into the sedimentary record. We carry out a series of experiments using a general circulation model (GCM), a lake energy balance model and a lake water balance model to better understand the processes by which these orbital variations could have altered lake evaporation, on-lake precipitation and runoff from the lake's catchment. GCM simulations indicate significant differences in surface incident shortwave radiation between the two end-members of the precession cycle. These differences cause lake evaporation to be ~ 25% higher when perihelion occurs at the summer solstice. GCM simulations also indicate significant seasonal changes in the amount of precipitation between the two end-members, but no change in the annual mean precipitation. Preliminary experiments with a lake water balance model show that local effects such as changes in vegetation, in snowmelt runoff, or in the area of mudflats surrounding the lake could have a large impact on lake level. However, more data need to be collected to determine the importance of these effects. Our results challenge previous interpretations of paleoclimate that were based on geologic data and simple assumptions regarding the effects of orbital variations on the water balance of the lake. In particular, we find that (1) changes in shortwave radiation may have been more important than changes in temperature or moisture in causing lake level fluctuations and (2) changes in catchment and lake characteristics should be further examined. In order to make an accurate reconstruction of past climatic change from a lake level record, climate system processes and local non-climatic variables must be considered explicitly.

Keywords: cyclic sequences; Green River Formation; precession; salt lakes; water balance

1. Introduction

Sedimentary records from many ancient lakes document water level fluctuations with a recurrence interval similar to that of the earth's precession cycle (e.g., Glenn and Kelts, 1991; Roehler, 1993; Olsen and Kent, 1996). To explain these lake level changes, researchers have suggested that variations in the earth's orbit induced changes in the climate system, which in turn altered the balance of on-lake precipitation, lake evaporation and catchment runoff. However, little is known about the processes by which orbitally forced changes in insolation are transferred

* Corresponding author. Department of Geosciences, Gould-Simpson Building, University of Arizona, Tucson, AZ 85721, USA.
E-mail address: cmorrill@geo.arizona.edu (C. Morrill).

0921-8181/01/$ - see front matter
PII: S0921-8181(00)00084-9

through the climate system and into the sedimentary record of a lake. By identifying and understanding these processes, more accurate interpretations of terrestrial paleoclimate can be made from these lake level records.

The lacustrine Green River Formation (Eocene) of southwestern Wyoming contains a long (several million years) record of lake contractions and expansions thought to be caused by the earth's precession cycle (Roehler, 1993). This sedimentary sequence, deposited in a lake known as Lake Gosiute, is of special interest because it is one of only a few records of Eocene climate variability on the scale of tens of thousands of years. The Eocene is a particularly important interval of the geologic past because it is a time during which the Earth likely experienced significant greenhouse warming (e.g., Zachos et al., 1994; Sloan and Rea, 1995). Our goal is to identify and better understand the processes by which orbital motions may have altered the water balance of Lake Gosiute through changes in (1) on-lake precipitation, (2) lake evaporation, and (3) runoff from the lake's catchment. To do this, we carry out a series of experiments using a general circulation model (GCM), a lake energy balance model and a lake water balance model.

Researchers have used several approaches for modeling orbitally forced lake level change. Kutzbach (1980) and Benson (1981) used coupled lake energy and water balance models to estimate the climatic conditions necessary for particular lake levels in two Quaternary lakes. Kutzbach and Street-Perrott (1985) used a GCM and a lake water balance model to determine what climatic forcing was responsible for lake level variations in African lakes during the past 18 ka. Like these previous studies, we use several models. This is necessary because we have little quantitative information about variability in precipitation on the precessional time-scale, about evaporation from Lake Gosiute, and about changes in runoff. We use a GCM to learn about changes in precipitation and in variables that influence lake evaporation, a lake energy balance model to explicitly examine lake evaporation and a lake water balance model to investigate the sensitivity of lake level to changes in runoff from the drainage basin.

Two particular aspects of this study may improve paleoclimatic interpretations from the sedimentary record of Lake Gosiute and perhaps other lake systems. First, we examine the relative influence of three components of the lake's water balance in causing lake level fluctuations. We consider whether lake level fluctuations were primarily caused by changes in on-lake precipitation, lake evaporation or runoff from the drainage basin. Second, these results allow us to consider the spatial scale (e.g., regional, hemispheric) of the climate signal that was recorded in Lake Gosiute sediments. For our purposes, this information is critical for relating the Lake Gosiute record to other Eocene climate proxy records. In a larger context, the relative influences of global and regional climatic change, as well as the influence of non-climatic factors, are concerns for many proxy records.

The paper is organized as follows. First, we describe the geologic setting of Lake Gosiute and evidence for precessional forcing of the lake's water budget (Section 2). Section 3 contains model descriptions. Section 4 details results from two GCM experiments in which we examine precessional forcing of Eocene climate. Next, we present results from lake energy balance model experiments that examine the impact of precessional forcing on lake evaporation (Section 5). Section 6 presents our results from a lake water balance model that address the possible effects of changes in runoff from the lake's drainage basin and Section 7 contains discussion.

2. Geologic background

Lake Gosiute existed for several million years during the early to middle Eocene ($\sim$55 to 40 Myr ago) in the Green River Basin of southwestern Wyoming. The lake formed in a structural depression bordered by Laramide ranges (Fig. 1). Uplift of these ranges probably began during the Maastrichtian ($\sim$65–75 Myr ago) and continued intermittently until the middle Eocene (Dickinson et al., 1988; Dettman and Lohmann, 2000). Stable isotopic and paleobotanical evidence suggests that while Lake Gosiute was present, the basin floor was about 300 m in elevation and the surrounding mountains were 2 to 3 km higher (Norris et al., 1996; MacGinitie, 1969). The Laramide uplifts approximately define the lake's drainage basin, which is estimated to be $\sim$ 125,000

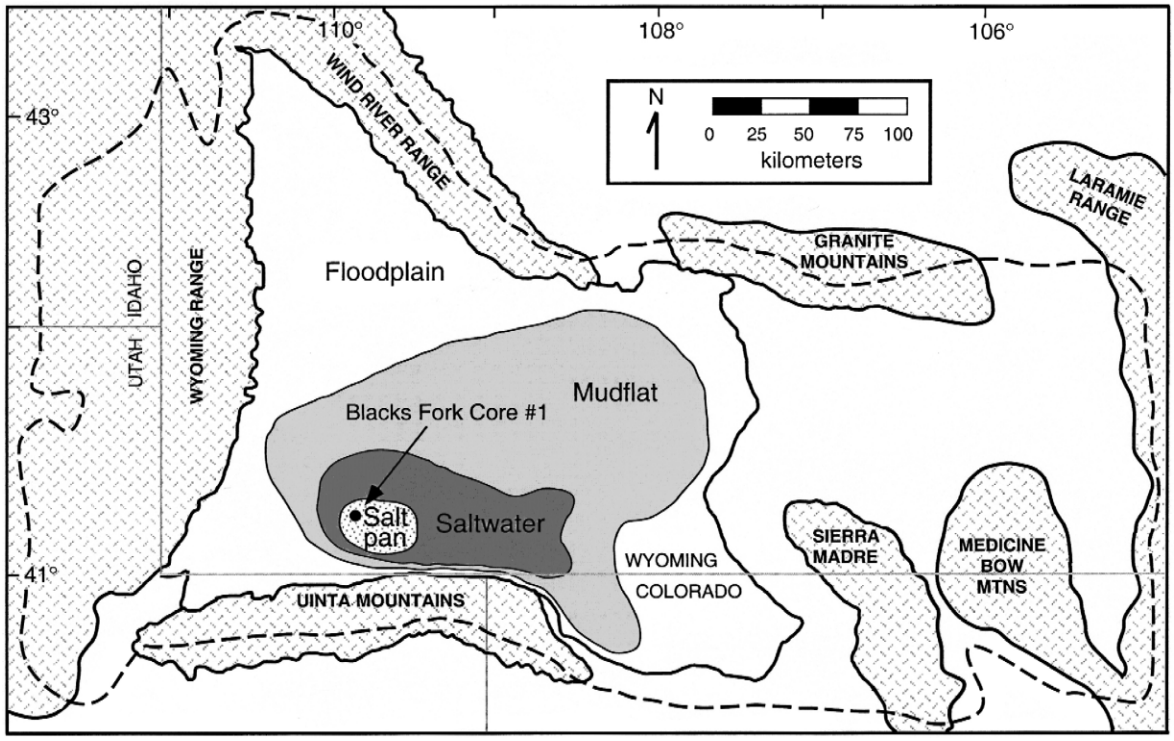

Fig. 1. Map of the present-day Green River Basin with facies present in a representative depositional cycle in the Wilkins Peak Member, after Roehler (1993). The saltwater and salt pan facies represent, respectively, maximum and minimum lake area. The dashed line marks the extent of the estimated Lake Gosiute drainage basin, after Bradley (1963). Circle indicates the source of the drill core section shown in Fig. 2.

km^2 (Bradley, 1963). Even though drainage basin area and paleoelevation are difficult to constrain for the Eocene, we use these estimates in our modeling experiments because they are the best available.

Sediments deposited in Lake Gosiute are preserved in the Green River Formation, which has several members corresponding to major lake high- and low-stands, each of which lasted several hundred thousand years or more. Evidence for precessionally forced lake level change occurs in the Wilkins Peak Member of the formation, which was deposited during a major low-stand (Roehler, 1993). During major lake high-stands, the lake drained to the south into Lake Uinta (Surdam and Stanley, 1980); however, during deposition of the Wilkins Peak Member, lake level was lower than the outlet and the lake was closed (Bradley and Eugster, 1964).

Cycles of lake expansion and contraction in the Wilkins Peak Member are manifested by a repeated sequence of lithologies, first described by Bradley and Eugster (1964). Lake high-stands are marked by oil shale layers, which are interpreted as perennial lake deposits. When the lake contracted and salinity increased, salt beds of trona or halite were deposited over the oil shale layers. Mudstones were deposited where subaerial mudflats expanded over the dried lake bed. Roehler (1993) identified 77 of these depositional cycles in cores from the Wilkins Peak Member (Fig. 2). Based on an estimated duration of 1.6 Myr for the member, he calculated an average period for the cycles of $\sim$21 kyr and suggested they were probably caused by the earth's precession cycle, which has periods of $\sim$19 and $\sim$23 kyr.

Several lines of evidence support the suggestion that orbital forcing caused the lake level changes preserved in the Wilkins Peak Member. First, sedimentary cyclicity on orbital time-scales (20–100 kyr) has been described in many settings during both

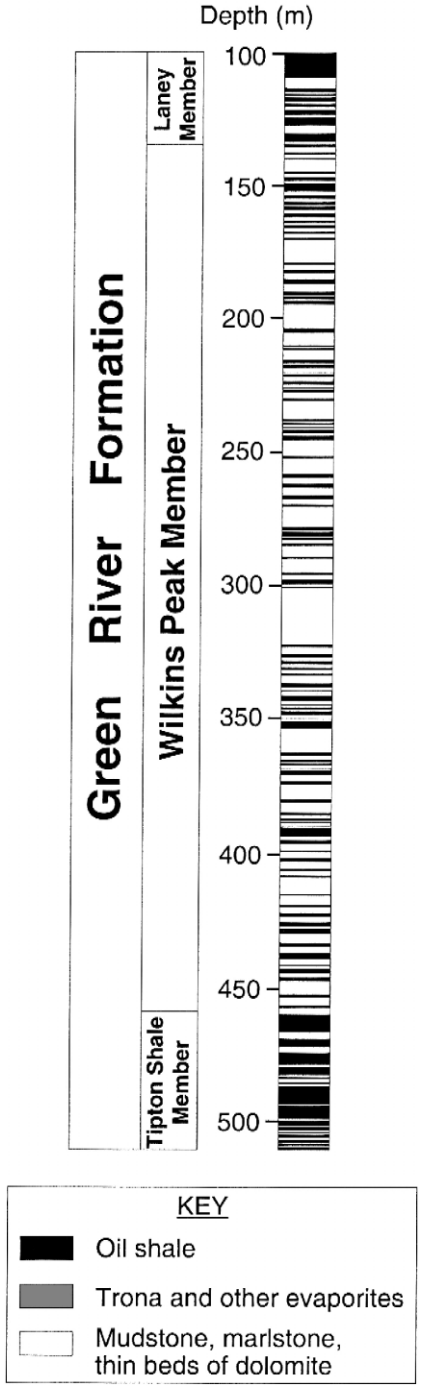

Fig. 2. Evidence for precessional forcing of Lake Gosiute's water balance from Energy Research and Development Administration Blacks Fork Corehole No. 1, after Roehler (1993). Location of the corehole shown in Fig. 1.

glacial and non-glacial time periods (e.g., Herbert and Fischer, 1986; Weedon and Jenkyns, 1990). Furthermore, Lake Gosiute existed in a continental interior, the setting with the largest thermal response to precessional forcing (Short et al., 1991). Last, there are lake sediments preserved in the Tipton Shale Member of the Green River Formation that also show evidence of orbital forcing. This member, deposited during a major high-stand preceding the Wilkins Peak Member, contains cycles of alternating organic-rich and organic-poor layers with a period of 19.5 kyr (Fischer and Roberts, 1991).

The evidence for precessional forcing of lake level changes preserved in the Wilkins Peak Member may be questioned for two reasons. First, the duration of the Wilkins Peak Member is uncertain. Roehler (1993) obtained an estimated duration of 1.6 Myr by calculating sedimentation rates from the dates of several volcanic tuffs near the top of the sequence and extrapolating these rates over the rest of the member. This approach may not be reliable because there are relatively large errors associated with the dates (Krishtalka et al., 1987), and sedimentation rates may vary through the member. Second, there is no evidence that the Lake Gosiute cycles are periodic rather than aperiodic. Aperiodic factors, such as tectonics and non-Milankovitch climate variability, could have driven the lake level changes (e.g., Carroll and Bohacs, 1999). There is good evidence for movement on nearby faults during Wilkins Peak time (Roehler, 1993), as well as for climate variability on several time scales (MacGinitie, 1969; Leopold and MacGinitie, 1972). Our model results provide a preliminary indication of whether orbital forcing can cause significant changes in the lake water balance and can, therefore, be a plausible cause of lake level fluctuations in Lake Gosiute.

3. Model descriptions

3.1. GENESIS GCM

We used version 2.0 of Global Environmental and Ecological Simulation of Interactive Systems (GENESIS), developed at the National Center for Atmo-

spheric Research. GENESIS consists of an atmospheric GCM (AGCM) interactively coupled to submodels of the mixed layer ocean, sea ice, land surface and soil (Fig. 3). This model's consideration of terrestrial physical, biophysical, and cryospheric processes makes it particularly useful for studying paleoclimate. Versions of GENESIS have been used in a number of paleoclimate simulations (e.g., Pollard and Schulz, 1994; Sloan and Rea, 1995; Pollard and Thompson, 1997).

Version 2.0 contains several improvements over an earlier version of this model (version 1.02). These include replacement of the single-effective-cloud layer with multiple cloud layers, additional cloud absorption of solar radiation, adjustments to the convective plume scheme, and higher spatial resolution. We use the standard version 2.0 resolution, which is spectral T31 ($\sim 3.75°$ lat $\times$ $3.75°$ lon) for the AGCM and $2°$ lat $\times$ $2°$ lon for the surface models. The AGCM has 18 vertical levels, tending from sigma coordinates near the ground to pressure coordinates at the top of the atmosphere. A more complete description of versions 2.0 and 1.02 and their differences can be found in Thompson and Pollard (1995, 1997) and Pollard and Thompson (1995).

The ocean submodel consists of a 50-m-deep thermodynamic slab that represents the ocean mixed layer. Sea surface temperature (SST) and seasonal heat storage vary due to changes in the surface energy balance; however, ocean circulation cannot change. Heat transport is calculated based on the present-day relationship between observed latitudinal SST gradient and zonal mean transport. Sea ice is represented by a three-layer thermodynamic model.

The land-surface model accounts for vegetation effects on near-surface fluxes of momentum, energy,

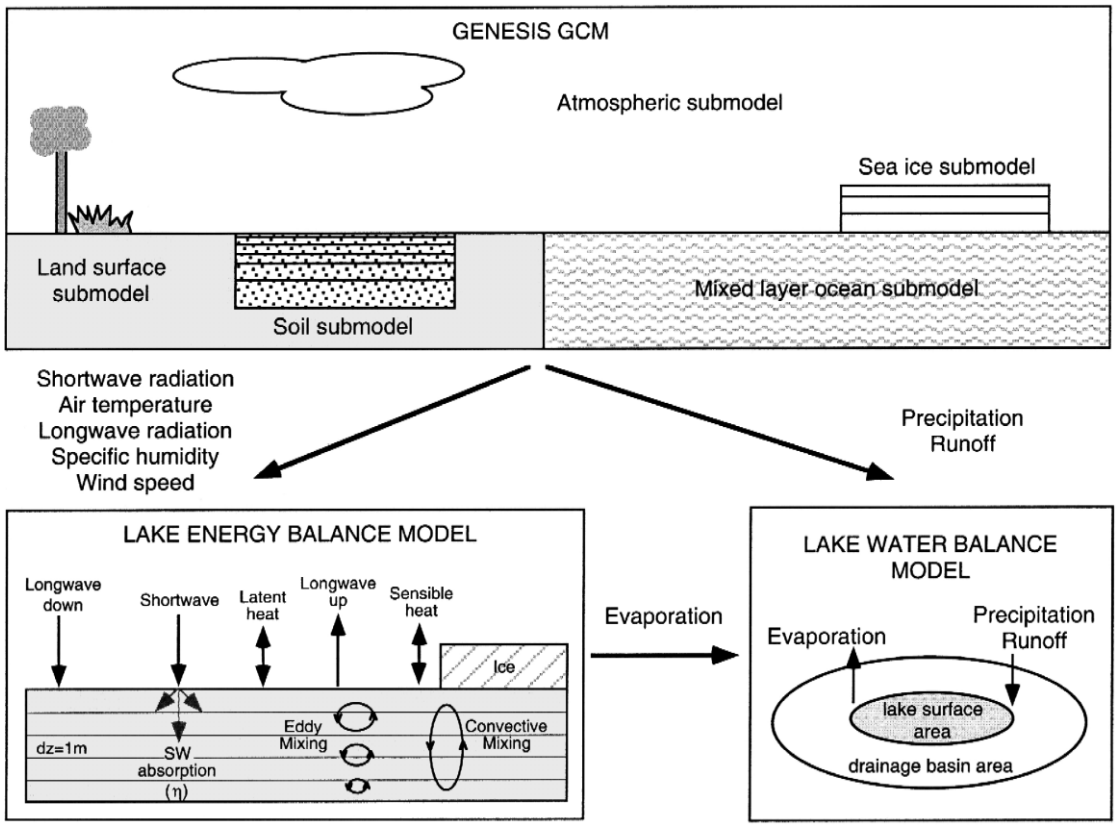

Fig. 3. Schematic illustration of the models described in the text. Arrows show the flow of output from one model to another.

and moisture. Up to two vegetation layers (upper canopy and lower canopy) can be included at each grid point. The soil submodel controls heat and moisture diffusion through the soil column. It consists of six layers, extending from the surface to 4.25-m depth. Surface runoff occurs when the rate of precipitation minus evaporation exceeds the infiltration rate of all soil layers. Water is allowed to drain from the bottom of the soil column; this flux represents near-surface runoff.

We carried out two GENESIS simulations representing the climatic end-members of a precession cycle. In one simulation (SMIN), perihelion occurs at the winter solstice and seasonality is at a minimum, and in the other simulation (SMAX), perihelion occurs at the summer solstice and seasonality is at a maximum. Because orbital parameters (i.e., eccentricity, precession, and obliquity) are not known for the Eocene, we rely on values calculated by Berger (1978) for the past five million years to specify orbital boundary conditions. From Berger's calculated timeseries, we select the precession cycle with the most extreme end-members in terms of insolation forcing at 45°N and use the orbital parameters (i.e., precession, obliquity, eccentricity) for that cycle's end-members as boundary conditions. It is reasonable to alter all three orbital parameters, even though our interest is the precession cycle, because all three parameters will change over the course of a precession cycle. Orbital specifications are given in Table 1 and Fig. 4 shows the Northern Hemisphere annual cycle of insolation in SMIN and SMAX.

We specify all other model boundary conditions identically for our two simulations. Eocene paleogeography (Fig. 5) is based on Scotese and Golonka (1992), with modifications by Sloan and Rea (1995). Topography is slightly modified from Sloan and Rea (1995); we have increased elevations as much as 600 m in western North America to agree more closely with estimates of large topographic relief (Fritz and Harrison, 1985; Norris et al., 1996; Dettman and Lohmann, 2000). Vegetation specification is unchanged from Sloan and Rea (1995) and is based on paleobotanical records. We set atmospheric carbon dioxide values at 560 ppm, which is based on results from Sloan and Rea (1995) and estimates from Cerling (1991), Freeman and Hayes (1992) and Sinha and Stott (1994).

Table 1
Orbital specifications

	SMIN	SMAX
Eccentricity	0.0531	0.0524
Precession[a]	90°	270°
Obliquity	22.8°	23.8°

[a] Measured as the prograde angle from perihelion to the vernal equinox.

3.2. Lake energy balance model

We use a one-dimensional lake energy balance model (Fig. 3) to determine what factors probably controlled evaporation from Lake Gosiute and also to derive evaporation estimates for our lake water balance model. This model was originally developed by Hostetler and Bartlein (1990), and was later modified by Small et al. (1999). Evaporation is dependent on the surface energy balance and vertical mixing, described below.

The lake surface energy balance is calculated as:

$$z\rho_w c_w \frac{\partial T}{\partial t} = \phi_s + \phi_{ld} - \phi_{lu} \pm Q_e \pm Q_h \pm M \qquad (1)$$

where z is the thickness of the surface layer (m), ρ_w is the density of water (kg m^{-3}), c_w is the specific heat of water (J kg^{-1} K^{-1}), T is surface water temperature (K), t is time, ϕ_s is shortwave radiation absorbed by the water surface, ϕ_{ld} is longwave radiation absorbed by the water surface, ϕ_{lu} is longwave radiation emitted by the water surface, Q_e is the latent heat flux, Q_h is the sensible heat flux and M is the energy flux due to mixing between the surface water and lower layers (units for all terms on the right-hand side of the equation are W m^{-2}). The amount of absorbed shortwave radiation is calculated from the lake surface albedo and values for surface incident radiation, which are taken from GCM output. Albedo varies as a function of solar zenith angle. The amount of absorbed longwave radiation is calculated from values of net upward longwave radiation taken from GCM output and values of upward longwave radiation (ϕ_{lu}), which are calculated from the lake surface temperature according to the Ste-

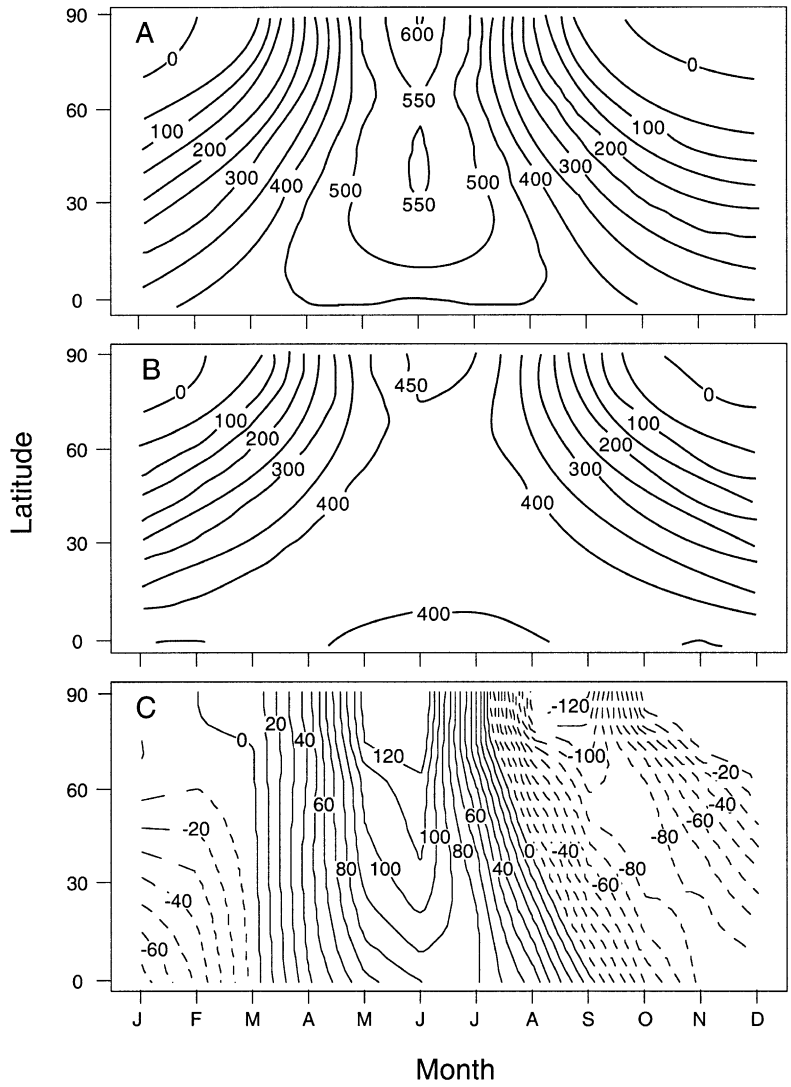

Fig. 4. Annual cycle of Northern Hemisphere insolation (W/m^2): (A) SMAX simulation, (B) SMIN simulation, (C) SMAX–SMIN. Solid lines indicate positive values and dashed lines indicate negative values.

fan–Boltzmann law. Latent and sensible heat fluxes are calculated using the standard bulk aerodynamic formulations of Dickinson et al. (1993):

$$Q_e = L_v \rho_a C_D V_a (q_s - q_a) \quad (2)$$

$$Q_h = c_p \rho_a C_D V_a (T_s - T_a) \quad (3)$$

where the subscripts a and s refer to air and surface, respectively, L_v is the latent heat of vaporization, c_p is the specific heat of air, ρ_a is the density of air, V_a is wind speed, and q is specific humidity. The momentum drag coefficient (C_D) is a function of (1) the neutral drag coefficient, which depends on the roughness length; and (2) the surface bulk Richardson number, which depends on the wind speed and the near-surface temperature gradient. Thus, the stability of the boundary layer affects evaporation, with unstable conditions leading to greater evaporation.

Vertical transfer of heat between layers in the lake ($dz = 1$ m) is accomplished through convective mixing and eddy and molecular diffusion. Convective

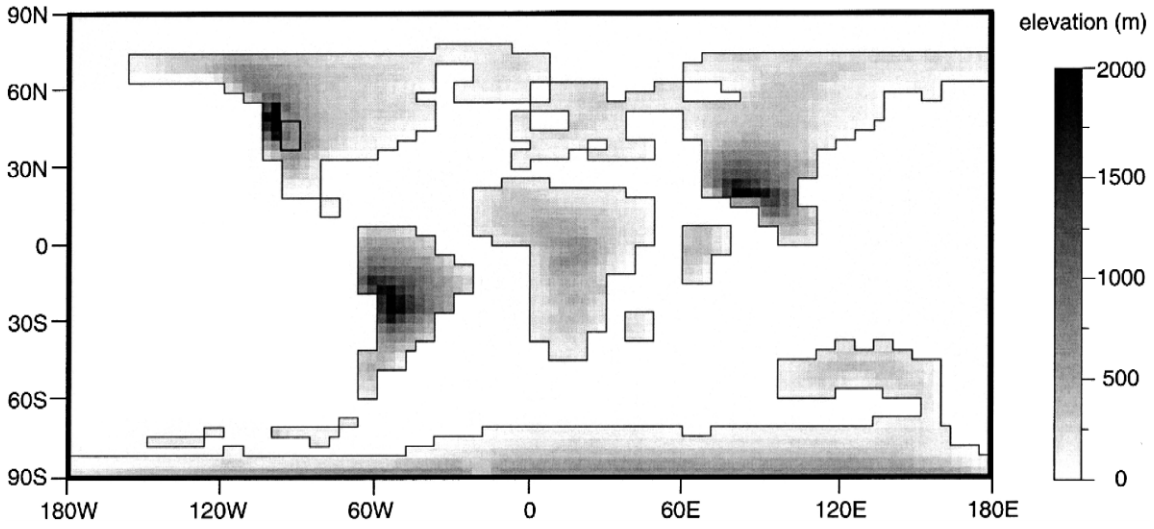

Fig. 5. Eocene paleogeography and topography used in the SMIN and SMAX simulations. Six grid-cell study area in western North America is outlined.

mixing occurs when there is an unstable density gradient (i.e., density decreasing with depth). It is the dominant form of mixing in the spring and fall. Eddy diffusion represents vertical transfer due to shear in the wind-induced water currents. Molecular diffusion is usually insignificant compared to eddy diffusion, but becomes important under ice and in deep parts (~ 10 m or greater) of the lake.

Salinity is constant through all layers of the lake. The lake model incorporates the effects of salinity on the density, specific heat and freezing point of water, as in Gill (1982). Increasing salinity also lowers the saturation vapor pressure, according to empirical relationships in Dickinson et al. (1965), thereby decreasing evaporation.

We drive the lake energy balance model with monthly averaged output for five variables (incident shortwave radiation, air temperature, specific humidity, longwave radiation, and wind speed) from our two GCM simulations. We linearly interpolate between monthly averaged output values to obtain input values for the lake energy balance model at a 30-min time-step. Experiments using modern meteorological measurements at several temporal resolutions (i.e., hourly, daily, monthly) indicate that the amount of annual lake evaporation estimated from monthly data interpolated to a 30-min time-step is accurate to within ~3% (not shown). This is the case because the thermal inertia of water prevents lake evaporation from changing greatly during short-term meteorological fluctuations (Pollard and Schulz, 1994). We input AGCM rather than surface values because land-surface values are governed by factors that do not directly affect the lake (e.g., vegetation, the low heat capacity of land relative to water). In order to correct for the difference in elevation between the GCM grid cells we use (~ 1100 m) and the estimated paleoaltitude of the lake (~ 300 m), we applied a local terrestrial lapse rate (6°C/km) calculated for the present-day western United States (Meyer, 1992) to air temperature values and adjusted specific humidity values in order to conserve relative humidity. In addition, we include in the lake model a method of interpolating lowest model sigma level (~ 50 m) values to values at 2 m above the lake surface. Our interpolation method generates a logarithmic profile that is dependent on boundary layer stability. This approach is based on that used in GENESIS to interpolate AGCM variables to the surface submodels.

The lake energy balance model and GCM do not interact, meaning output from the lake model does not influence the meteorological variables driving it. This approach is probably reasonable in regards to precipitation, runoff and radiation because the volume of evaporation from Lake Gosiute was likely

too small to significantly affect large scale variables such as cloud cover and rainfall. However, a lake of the size of Lake Gosiute would likely affect air temperature, specific humidity and wind speed. These effects are not represented in our method. We discuss the potential shortcomings of our approach below.

3.3. Lake water balance model

We calculate changes in lake surface area by assuming the lake is in hydrological equilibrium with climate conditions and solving the steady-state lake water balance equation at each climatic end-member of the precession cycle. This is a reasonable assumption because we are considering the impact of gradual climate change on a lake with a short hydrologic response time (~ 5 years, calculated using the equation of Mason et al., 1994). The steady-state lake water balance equation is derived from the following equation for the water balance of a closed lake:

$$\frac{\mathrm{d}z}{\mathrm{d}t} = P_{\mathrm{L}} - E_{\mathrm{L}} + R\frac{A_{\mathrm{B}}}{A_{\mathrm{L}}} \quad (4)$$

where z is mean lake depth, P_{L} is on-lake precipitation (m/year per unit lake area), E_{L} is lake evaporation (m/year per unit lake area), R is runoff (m/year per unit area basin area), A_{B} is drainage basin area, and A_{L} is lake surface area. In Eq. (4), we assume that the net groundwater flux into or out of the lake was probably minimal. This is a reasonable initial assumption, although it is likely that groundwater fluxes into the lake were non-negligible when lake levels were low (Eugster, 1971). Assuming the lake is in hydrologic equilibrium, we rearrange Eq. (4) to obtain the following steady-state solution for lake level:

$$A_{\mathrm{L}} = \frac{RA_{\mathrm{B}}}{(E_{\mathrm{L}} - P_{\mathrm{L}})} \quad (5)$$

We use Eq. (5) to calculate the lake level at each of the two climatic end-members of the precession cycle.

4. GCM results

We use GCM experiments to understand how climatic parameters important to Lake Gosiute's water budget might change due to precessional forcing. We examine GCM output for six grid cells in western North America (Fig. 5) that are centered on the estimated location of Lake Gosiute (lat centered on 46°N, lon centered on 95°W). We use several grid cells in order to minimize noise that is associated with values from individual grid cells. Both the SMAX and the SMIN simulations were initiated from an equilibrated Eocene simulation of 16-year duration that incorporated modern orbital parameters. The SMAX and SMIN simulations were each 15 years long and equilibrium was reached within several years. Below, we report values averaged over the final five simulation years for shortwave radiation, precipitation and runoff. Changes in other variables affecting the hydrologic budget of the lake (air temperature, specific humidity, longwave radiation and wind speed) do exist; however, we find that these changes do not significantly influence lake evaporation, as discussed in Section 5.

4.1. Shortwave radiation

The SMAX case has significantly higher summer (April to August) and lower winter (September to January) surface incident shortwave radiation than the SMIN case (Fig. 6A). This is expected given the differences in solar radiation at the top of the atmosphere that result from our specification of orbital parameters (Fig. 4). There is little change in cloudiness between the two simulations.

4.2. Precipitation

Annually, the region surrounding Lake Gosiute receives the same amount of precipitation in the SMAX and SMIN simulations. There are, however, significant seasonal differences. Rainfall in the six grid-cell study area, like that in other locations in the mid-latitudes, is dominated by frontal storms in the winter and convective precipitation in the summer. In each simulation, the amount of summer convec-

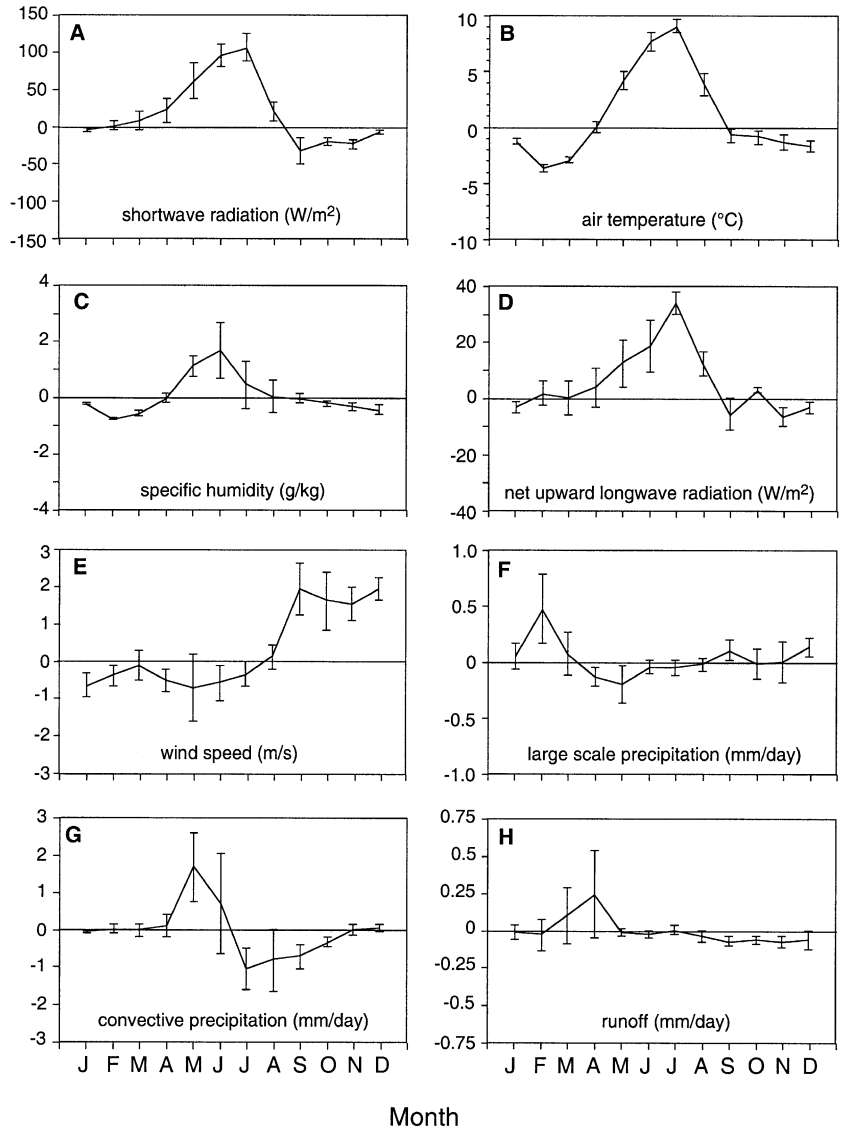

Fig. 6. Monthly averaged difference (SMAX–SMIN) over the six grid-cell study area in: (A) surface incident shortwave radiation, (B) air temperature ($\sigma = 0.993$), (C) specific humidity ($\sigma = 0.993$), (D) net upward longwave radiation, (E) wind speed, (F) large-scale precipitation, (G) convective precipitation, (H) runoff. Error bars represent 95% confidence intervals for the difference.

tive precipitation is about three times larger than the amount of winter large-scale precipitation.

We interpret the differences in winter precipitation (December to March) between the two cases as follows. The pole-to-equator temperature gradient is reduced in the SMAX case relative to the SMIN case by as much as 9°C (not shown). There are two primary sources of this change. First, high-latitude sea ice is reduced in the SMAX case, resulting from warmer summer temperatures in this simulation. Second, the difference in insolation from low to high latitudes is less in the SMAX case (Fig. 4). The lower temperature gradient in the SMAX simulation yields weaker mid-latitude baroclinic waves. Over North America, the amplitudes of both the climatological troughs over the north Pacific and the north

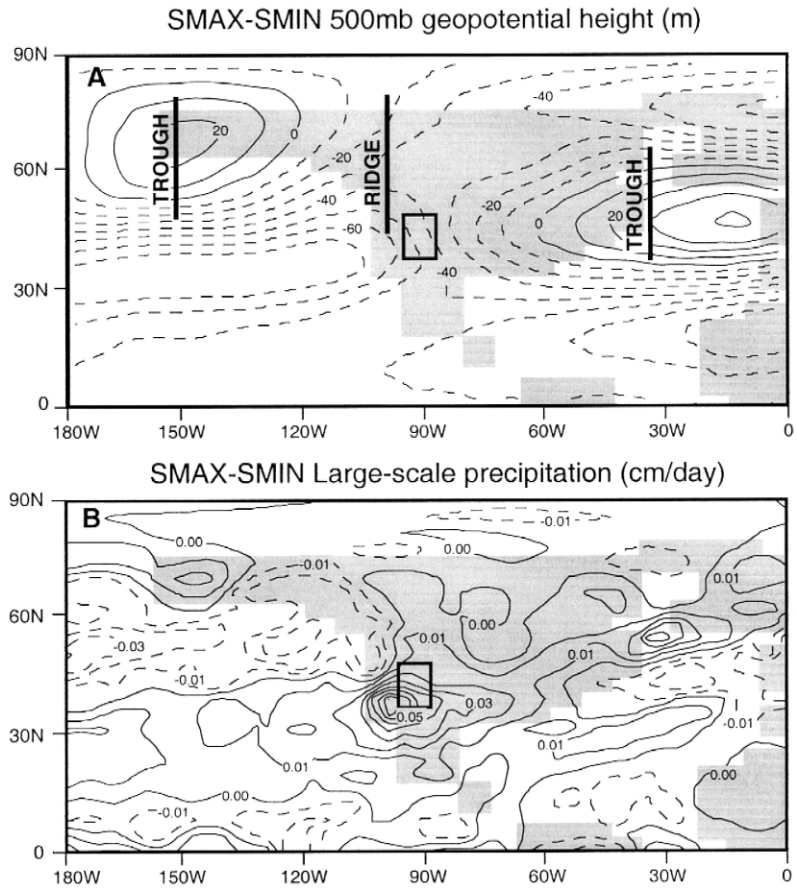

Fig. 7. Difference (SMAX–SMIN) in December–January–February–March (A) 500 mb geopotential height (m), and (B) large-scale precipitation (cm/day). Box shows six grid-cell study area. Solid lines indicate positive values and dashed lines indicate negative values. Thick solid lines in (A) show the locations of trough and ridge axes.

Atlantic and the climatological ridge over western North America decrease (Fig. 7A). The more zonal flow in the SMAX simulation results in reduced precipitation in trough areas (e.g., north Atlantic; Fig. 7B) and enhanced precipitation in ridge areas (e.g., western North America; Fig. 7B), as trough and ridge areas are associated with upper-level divergence and convergence, respectively.

The SMAX case also receives more May and June convective rainfall and less July to October convective rainfall than the SMIN case (Fig. 6F). In this GCM, differences in convective precipitation are caused by changes in the vertical gradient in moist static energy (i.e., the vertical gradient in the sum of the sensible and latent heat contents of air). Orbital forcing affects the vertical gradient in moist static energy primarily through changes in surface radiation and evaporation. In May and June, the SMAX case has greater surface heating, which results from greater surface net radiation relative to the SMIN case (Fig. 8). Greater surface heating leads to higher surface temperatures, which increase the vertical gradient in moist static energy (not shown) and increase convection. In July and August, near-surface soil moisture is substantially lower in the SMAX case due to significant losses through evaporation during the preceding several months (Fig. 8). The loss of surface moisture in the SMAX case decreases the vertical gradient in moist static energy and makes the boundary layer more convectively stable. In Septem-

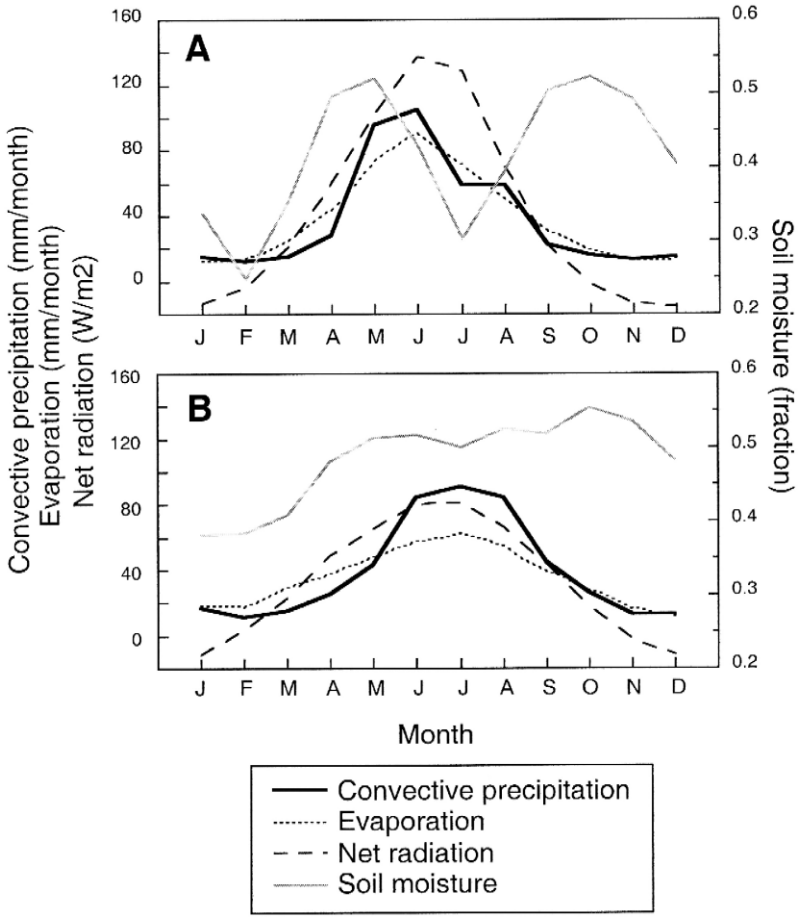

Fig. 8. Monthly averaged values for convective precipitation (mm/month; solid black line), evaporation (mm/month; dotted black line), net radiation (W/m^2; dashed black line), and moisture in the uppermost 5 cm of soil (fraction of liquid volume relative to ice-free pore space; solid gray line) for the (A) SMAX and (B) SMIN simulations.

ber and October, convective precipitation is lower in the SMAX case than in the SMIN case due to lower surface net radiation.

4.3. Runoff

Annually, runoff in the region surrounding Lake Gosiute does not change between the SMAX and SMIN simulations. There are, however, significant seasonal differences. The largest change occurs in the spring, when the SMAX case has significantly higher March and April runoff than the SMIN case (Fig. 6G). This results from greater winter snowfall and spring snowmelt in the SMAX case. Other changes in runoff are associated with precipitation changes, though they lag these changes by at least a month. This lag is caused by sub-surface runoff, which moves slowly through the soil column. Most notably, runoff is greater in the SMIN case from August to December, following greater July to October convective precipitation.

5. Lake energy balance model results

Our primary goal in this section is to determine how evaporation from Lake Gosiute might have differed at the two climatic end-members of the precession cycle and which climate parameter changes are responsible for this difference. In addi-

tion, we consider the sensitivity of evaporation to several lake boundary conditions that we must specify. We use these sensitivity studies to identify if changes in boundary conditions through time will have a considerable influence on evaporation and if the initial values we choose will have a significant impact on our results. The results we present below are derived from 10-year lake model integrations. We exclude results from the first 5 years to allow for model equilibration.

5.1. Climatic forcing of lake evaporation

We first carry out two lake energy balance model experiments in which all climatic inputs are set to (1) values obtained from the SMIN GCM simulation and (2) values obtained from the SMAX GCM simulation. Results from these two experiments show that annual lake evaporation is higher for climatic forcing from the SMAX simulation (Table 2). To determine which of the climate inputs are responsible for this difference, we carry out five additional lake model experiments. In each of these experiments, a different climate variable is set to values obtained from the SMAX simulation, while the remaining four climate parameters are set to values obtained from the SMIN simulation. Results from these experiments indicate that shortwave radiation is responsible for most of the annual evaporation difference between the two climatic end-members (Table 2).

Table 2
Impact of orbitally induced change in climate parameters on lake evaporation

	Evaporation (cm/year)	Change from all SMIN (cm/year)
All parameters set to SMIN values	65.6	–
All parameters set to SMAX values	84.7	19.1
All parameters set to SMIN values except		
Shortwave radiation set to SMAX value	81.5	15.9
Air temperature set to SMAX value	70.4	4.8
Specific humidity set to SMAX value	68.2	2.6
Longwave radiation set to SMAX value	60.2	−5.4
Wind speed set to SMAX value	66.6	1.0

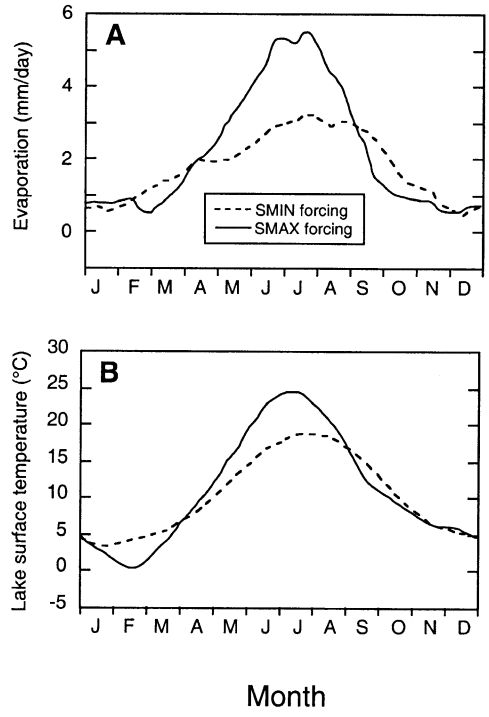

Fig. 9. Annual cycle of (A) evaporation (mm/day) and (B) lake surface temperature (°C) from lake energy balance model experiments in which the effects of changes in shortwave radiation are isolated. Solid lines indicate experiments in which shortwave radiation is set at values obtained from the SMAX GCM simulation and dashed lines indicate experiments in which shortwave radiation is set at values from the SMIN GCM simulation.

When shortwave radiation inputs to the lake energy balance model are changed from SMIN to SMAX values, summer evaporation increases and winter evaporation decreases (Fig. 9A). The change in summer (winter) evaporation is due to an increase (decrease) in shortwave radiation, which leads to warmer (colder) lake surface temperatures (Fig. 9B). The increase in evaporation during the summer more than offsets the decrease in evaporation during the winter, however, because evaporation increases exponentially with lake surface temperature. The difference in evaporation caused by changes in shortwave radiation from the SMIN to SMAX end-members is ~25%.

Changing specific humidity and air temperature inputs from SMIN to SMAX values also results in higher annual lake evaporation, although the changes are relatively small. Increased summer air temperature in the SMAX case causes increased sensible heating of the lake surface and an increase in annual lake evaporation. Specific humidity changes affect evaporation through the lake-to-air specific humidity gradient (Eq. (2)). SMAX values for this parameter lead to a higher gradient during the winter, which increases overall annual evaporation.

Changing longwave radiation inputs from SMIN to SMAX values results in lower annual lake evaporation due to a decrease in summer evaporation. Summer net longwave radiative cooling is greater in the SMAX case than in the SMIN case, translating into a greater loss of radiant energy from the lake and a decrease in evaporation when SMAX values are used as input. However, the change in net longwave radiation obtained from the two GCM simulations should be treated as a maximum estimate of the change in this variable. This is the case because the GCM uses land-surface temperature, rather than lake-surface temperature, to calculate longwave radiation emitted from the surface. Lake surface temperature changes much less than land-surface temperature between the two simulations due to the greater heat capacity of water.

Wind speed has little effect on annual evaporation because the differences between SMIN and SMAX values for this parameter are small (≤ 1 m/s). In addition, spring/summer evaporation changes cancel fall evaporation changes because they are in the opposite direction. However, the GCM only simulates changes in large-scale winds and we have not considered local changes in wind speed due to lake breezes or downslope winds from the surrounding mountains. These could be significant, but are beyond the scope of this research.

5.2. Sensitivity of evaporation to lake boundary conditions

The lake energy balance model requires values for salinity, depth and shortwave extinction coefficient (η). We specify plausible ranges for these variables based on geological interpretations of the Wilkins Peak Member and carry out a series of sensitivity studies to determine how specification of these variables affects evaporation.

Our upper bound for salinity (300 ppt) is the value required for trona to precipitate (Bradley and

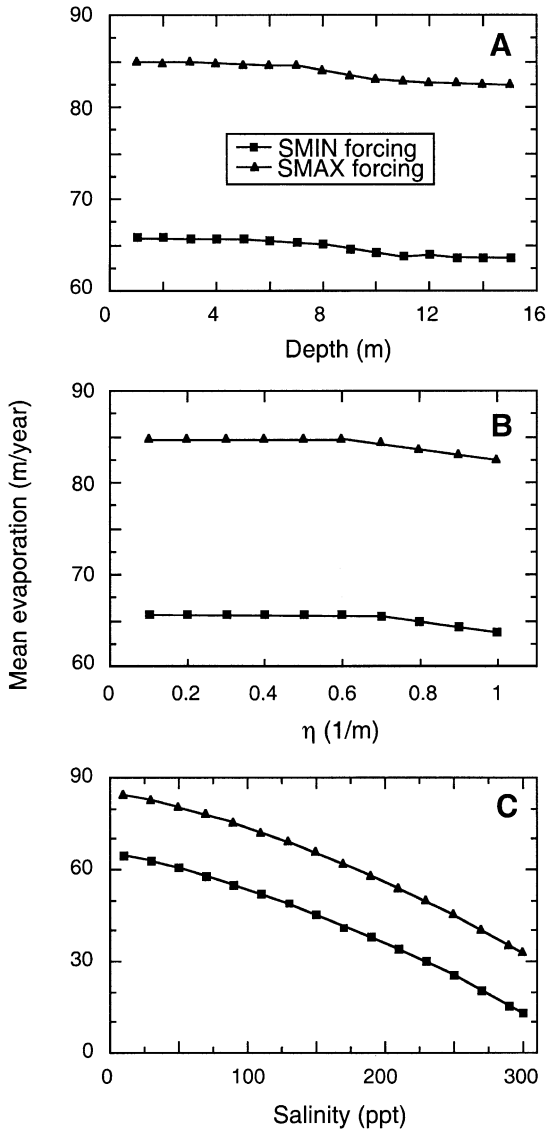

Fig. 10. Sensitivity of lake evaporation to changes in (A) lake depth, (B) shortwave extinction coefficient (η), and (C) salinity. Squares and triangles indicate a single steady-state lake model simulation. Squares represent simulations with all climatic variables set to values from the SMIN GCM simulation, triangles represent simulations with all climatic variables set to values from the SMAX GCM simulation.

Eugster, 1964), and our lower estimate (5 ppt) is chosen to reflect the salinity tolerated by organisms (e.g., fish, gastropods, ostracodes) found in parts of the Wilkins Peak Member (e.g., Roehler, 1993). We choose lake depths (1 to 15 m) that are shallow enough for light to penetrate to the lake bottom, a condition necessary for the photosynthetic organisms thought to have lived on the lake bottom (Bradley, 1973; Eugster and Hardie, 1975; Smoot, 1983). Values of η for Lake Gosiute are less constrained, so we choose a range (0.1–1.0 m^{-1}) that includes measurements from many present-day shallow and biologically productive lakes.

Of these three variables, annual evaporation is by far most sensitive to salinity changes. Changing salinity by $\sim$30 ppt affects evaporation as much as varying depth or η over their entire range of possible values (Fig. 10). In addition, changes in depth or η lead to a small change in evaporation relative to that caused by orbitally induced climate change. However, the evaporation decrease due to rising salinity is significant relative to the difference in evaporation simulated between the two climatic end-members (Table 2). A change in salinity of the order of 150 ppt will lead to a change in evaporation that is similar in magnitude to the simulated change due to variations in shortwave radiation between the SMIN and SMAX end-members. Because ice does not form on Lake Gosiute in any of our simulations, salinity affects evaporation solely through a change in surface saturation vapor pressure. As salinity increases, the surface saturation vapor pressure decreases, reducing the lake-to-air specific humidity gradient and reducing evaporation (Fig. 11). The variations in lake evaporation due to lake depth and η result from differences in the depth to which incident shortwave radiation penetrates, which impact the annual surface temperature cycle of the lake.

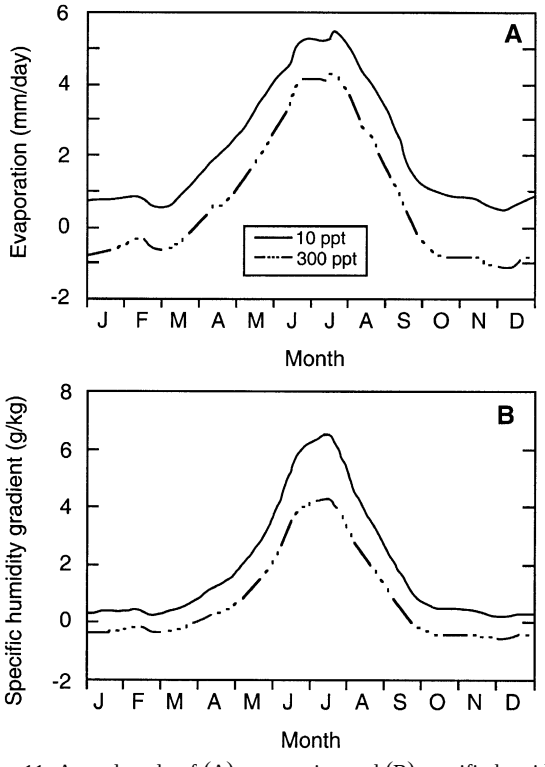

Fig. 11. Annual cycle of (A) evaporation and (B) specific humidity gradient ($q_s - q_a$) in two lake model simulations. Solid line is low salinity (10 ppt) and dash-dot line is high salinity (300 ppt).

6. Lake water balance model results

Results from GCM and lake energy balance model experiments suggest that a maximum in evaporation and a minimum in lake level occurred at the SMAX end-member. Salinity changes could dampen the lake level response to evaporation change, however, with a salinity increase of $\sim$150 ppt causing a decrease in evaporation that is similar in magnitude to the increase in evaporation caused by orbitally forced shortwave radiation changes. These results suggest that, as long as large changes in salinity do not occur, orbital forcing could greatly impact the lake water balance through changes in lake evaporation. Our models do not provide a perfect representation of the lake and climate systems, however. In particular, there are several processes that influence runoff that the GCM either does not include or does not represent well. In this section, we investigate the effects of some of these processes by using a simple lake water balance model. Data relevant to these processes are sparse, so these modeling efforts are speculative. However, these results identify processes that should be addressed in future research.

There are several processes that influence runoff that might require further consideration. First, vegetation does not vary in the GCM between the two precessional end-member cases. In both cases, we have prescribed vegetation to be broadleaf shrubs,

which is consistent with Eocene paleobotanical records of this area (MacGinitie, 1969; Wilf, 2000). However, given the large seasonal changes in temperature and precipitation seen between the GCM simulations, it seems likely that vegetation changed over the course of the precession cycle. Studies in modern-day systems (e.g., Sorrisovalvo et al., 1995; Cerda, 1996) show that vegetation changes can induce changes as large as ~0.3 in the runoff coefficient (i.e., the ratio of runoff to precipitation). Unfortunately, there are no data on vegetation changes on the precessional time scale in this region. Therefore, we do not know what vegetation changes, if any, occurred in this region over the course of the precession cycle.

Second, GCM grid cells are too large to resolve the high mountains that are thought to have existed in western North America during the Eocene (Fritz and Harrison, 1985; Norris et al., 1996; Dettman and Lohmann, 2000) and the GCM may therefore underestimate the amount of runoff from spring snowmelt. GCM results show a large difference in snowmelt runoff between the two cases with the SMAX case, which is colder and wetter during the winter, having greater spring runoff. It is possible that the difference between the simulations could be either amplified or dampened if the model incorporated large mountains surrounding the basin. Again, there are few data on temporal variations in the amount of snow and snowmelt runoff. Isotopic work by Norris et al. (1996) show possible temporal variations in the amount of snowmelt entering Lake Gosiute during deposition of the Wilkins Peak member, but these variations could result from diagenetic alteration (Morrill and Koch, 1999).

Third, evidence from the geologic record suggests that mudflats and small ephemeral lakes formed in the areas that were exposed during regression of Lake Gosiute (Eugster and Hardie, 1975; Smoot, 1983). Expansion of mudflats and playas could have had a significant impact on the transfer of runoff from the basin into the lake. For instance, some of the runoff flowing into these areas from the basin might have been trapped in playas, where it evaporated and therefore never reached Lake Gosiute. In addition, the mudflats might have altered the relative proportions of overland flow, groundwater flow and channel flow. These changes could also have altered the amount of runoff lost to evaporation and could have caused either an increase or decrease in the amount of runoff delivered to the lake. It is unknown, however, to what extent these changes modified the amount of runoff entering Lake Gosiute.

To examine the impacts of changes in runoff coefficient between the two precessional end-members, we have completed a series of calculations using the lake water balance equation (Eq. (5)). For comparison, we have also calculated the percent lake area change caused by changes in lake evaporation. These calculations require knowledge of the drainage basin area, which is not well known. As discussed earlier, Bradley (1963) estimated the drainage basin area to be ~125,000 km^2, or roughly 10 times the area of Lake Gosiute at its highest Wilkins Peak levels (Roehler, 1993). We use this as our best estimate of drainage basin area, but also show calculations for drainage basin areas an order of magnitude smaller and larger in order to give an indication of the error associated with these calculations.

Fig. 12 shows the results of our water balance calculations. Using a runoff coefficient of 0.35 obtained from the GCM simulations and an initial ratio of drainage basin area to lake area of 10 (i.e., $A_B/A_L = 10$), the ~25% increase in lake evaporation modeled between the SMIN and SMAX endmembers leads to a decrease in lake area of ~25% (Fig. 12A). An equivalent change in lake area is caused by a decrease in the runoff coefficient of ~25% (e.g., from 0.35 to 0.26; Fig. 12B). Because a ~25% change in the runoff coefficient is plausible, these calculations suggest that changes in the runoff coefficient could be as important as changes in lake evaporation to the lake water balance. Calculations for $A_B/A_L = 1$ and $A_B/A_L = 100$ show that lakes with a relatively large drainage basin are more sensitive than lakes with a small drainage basin to changes in the runoff coefficient. This is the case because a decrease (increase) in the runoff coefficient leads to a larger absolute decrease (increase) in the volume of runoff generated in a large basin. Conversely, lakes with a relatively large drainage basin are less sensitive than lakes with a small drainage basin to changes in lake evaporation. This is the case because changes in evaporation cause changes in lake surface area that alter the depth of runoff added to the lake per unit of lake surface area.

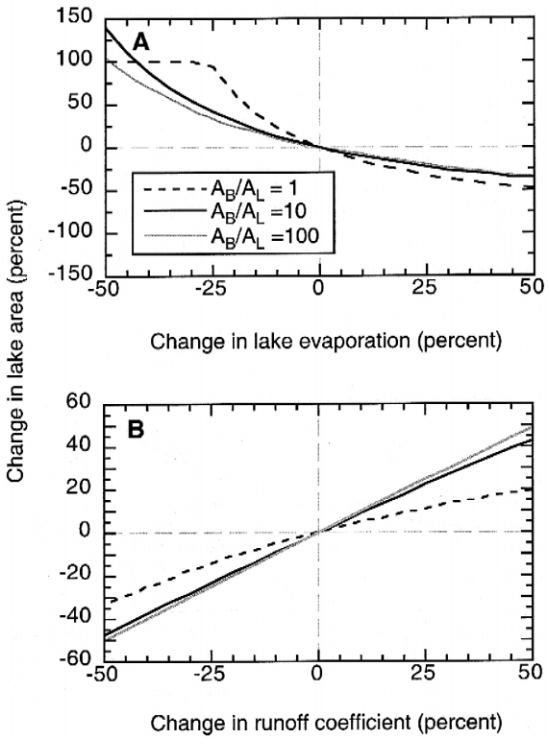

Fig. 12. The percent change in lake area resulting from (A) percent change in lake evaporation and (B) percent change in runoff coefficient (runoff/precipitation). Dotted black line indicates A_B / A_L (drainage basin area/lake area) of 1, black line indicates A_B / A_L of 10, and gray line indicates A_B / A_L of 100. The percent change in lake area cannot be larger than 100% for an A_B / A_L of 1 because the lake would overflow at that level.

This change in the depth of runoff, which counteracts the lake level fluctuation, is greater for large drainage basins because these catchments generate more runoff.

Given the uncertainties in both our model experiments and the geologic data, the magnitude of the lake area changes obtained by these lake water balance calculations is reasonable. Our model results suggest that lake surface area decreased by 25% at the SMAX end-member due to changes in lake evaporation, while Roehler (1993) suggested lake area changes on the order of 50–75% based on mapping of lake deposits. However, the lake water balance calculations also show that changes in the runoff coefficient between the two precessional end-members have the potential to substantially impact the lake water budget. In particular, if the runoff coefficient were to increase from the SMIN to the SMAX end-member, lake level minima might occur at the SMIN end-member. Our best guess is that lake level minima occurred at the SMAX end-member due to changes in lake evaporation driven by changes in shortwave radiation. However, it is critical to obtain more field data about changes in vegetation, the amount of snowmelt runoff, and mudflat and playa paleoenvironments in order to assess the importance of changes in the runoff coefficient.

7. Discussion

We have examined some of the processes by which orbital forcing may have altered the water balance of Lake Gosiute. Our goals were to provide more accurate paleoclimate interpretations of Lake Gosiute water level fluctuations and also to consider the spatial scale (e.g., local, regional, hemispheric) of the climate signal that may have been recorded in Lake Gosiute sediments. By investigating these processes, we might also be able to provide insight into the hydrologic response of other lake systems to climate change.

Previous climatic interpretations of Lake Gosiute water level fluctuations suggest that lake level maxima occurred during warm and humid periods of the precession cycle and lake level minima occurred during hot and arid periods (Roehler, 1993; Matthews and Perlmutter, 1994). Our results question several assumptions on which these interpretations are based, as discussed below, and indicate that it is essential to explicitly consider the specific processes involved in climatic and lake level change for a given lake system.

First, our GCM simulations indicate that, during a precession cycle, temperature and moisture do not necessarily change in opposite directions. We find large changes in temperature between the two simulations, but no change in annual precipitation. It is possible, however, that the GCM does not accurately model precipitation changes, particularly because this variable has high spatial variability and depends on the parameterization of sub-grid scale processes. Experiments with other models, especially those with different convective or large-scale precipitation schemes, might yield different results. If precipitation were to change between the two climatic end-

members, it is perhaps more likely that temperature and precipitation would change in the same direction. Other studies of past and future climate change indicate that these two parameters often positively covary (e.g., Manabe and Wetherald, 1975; Barron et al., 1989). Further work is needed, both in modeling experiments and field data collection (e.g., Wilf et al., 1998), to better constrain precipitation changes.

Second, GCM results show that temperature and moisture differences between the two cases vary seasonally, and neither end-member is consistently warmer or more humid than the other. For example, summer temperatures are higher in the SMAX simulation than in the SMIN simulation, but winter temperatures are colder. In addition, precipitation is greater in the winter and spring in the SMAX simulation, but precipitation is greater in the summer and fall in the SMIN simulation. These seasonal differences are expected given the seasonality of the insolation changes (Fig. 4).

Third, our results suggest that shortwave radiation changes play a larger role than temperature or precipitation change in determining lake evaporation and lake level change. We should note, however, that Bowen ratios ($B = Q_h/Q_e$) in our lake model experiments are ~ 0.3, which are significantly higher than the values typical for lakes (~ 0.1; Kutzbach, 1980) and suggest that sensible heating of the lake surface is overestimated and/or lake evaporation is underestimated in our experiments. If sensible heating is overestimated, the most likely cause is the inability of lake surface temperature to impact air temperature in our stand-alone model. If this is the case, air temperature effects on evaporation, which result from sensible heating of the lake surface, are also overestimated. Alternatively, lake evaporation may be underestimated in our experiments because values calculated by GENESIS v. 2.0 for shortwave radiation tend to be too low. Values for surface incident shortwave radiation in western North America from a present-day control run (e.g., ~ 200 W/m^2 in July; Pollard, personal communication) are significantly lower than observed values (~ 300 W/m^2; Sellers, 1965). This has important implications for using GCMs to understand the effects of precessional forcing on a lake's water balance. Most GCMs, including GENESIS, do not accurately simulate the impact of clouds on surface incident shortwave radiation. If shortwave radiation is the climate parameter that most greatly impacts lake evaporation, we may not be able to accurately model the effects of insolation changes on the lake water balance. Nevertheless, our results suggest that the impact of shortwave radiation change, and not just that of air temperature and moisture change, on evaporation should be considered.

Fourth, previous interpretations make no mention of the potential importance of changes in catchment or lake characteristics (e.g., vegetation change or changes in salinity). Though our results in these areas are still speculative due to lack of field data, it appears plausible that changes in the runoff coefficient and/or lake salinity could impact lake level change. Changes in catchment characteristics are especially important because they might determine the timing of lake level minima and maxima relative to precessional forcing. For example, lake level maxima could occur at the SMAX end-member, despite greater lake evaporation, if this end-member experienced a large increase in snowmelt runoff from surrounding mountains or a change in vegetation type or density that led to less interception of precipitation. Salinity changes could be very important because they could greatly dampen lake level fluctuations induced by changes in lake evaporation or catchment characteristics.

The second goal of this research was to use our modeling results to consider the spatial scale of the climate signal that may have been recorded in Lake Gosiute sediments. GCM results indicate that climate parameters that respond closely to insolation forcing (i.e., shortwave radiation and air temperature) change similarly throughout the Northern Hemisphere. Thus, evaporation changes caused by variations in shortwave radiation are likely indicative of hemispheric changes in shortwave radiation. In contrast, climate parameters affected by circulation changes and internal climatic feedback processes (e.g., high-latitude sea ice changes) differ regionally. For example, winter precipitation increases from the SMIN to the SMAX simulation in western interior North America, but winter precipitation decreases between the two simulations in the Pacific Northwest (Fig. 7). In addition, changes in catchment vegetation or in the amount of snowmelt runoff from surrounding mountains could add a local signal to the Lake Gosiute

sedimentary record. The importance of precipitation changes and changes in catchment characteristics must be known before we can determine how much information the sedimentary record of Lake Gosiute provides about climate in regions other than western North America.

Several of our findings may be applicable to other lake systems. First, lake energy balance model results suggest that changes in shortwave radiation can have a large impact on the lake water balance. Many previous studies, such as those mentioned above, interpret lake level fluctuations solely in terms of temperature and moisture changes. Because air temperature and shortwave radiation changes often positively covary, lake level changes previously interpreted in terms of temperature change could perhaps have been partially forced by changes in shortwave radiation. Second, results from a simple lake water balance model illustrate the importance of changes in the runoff coefficient. This variable may sometimes be overlooked when interpreting lake level change. In conclusion, our results illustrate a number of complex atmospheric processes and local, catchment processes that can control lake level change. Simple climatic interpretation of lake level change without consideration of these processes may result in inaccurate reconstructions of past climatic change.

Acknowledgements

We thank Paul Koch and Scott Wing for their helpful comments on an earlier draft and Dave Pollard for providing technical advice, GENESIS code, and results from a present-day simulation. The comments of two anonymous reviewers led to many improvements in the paper. This material is based upon work supported under a National Science Foundation Graduate Fellowship to CM. LCS acknowledges NSF (ATM-9627795) for support of this research. Computing was carried out at the National Center for Atmospheric Research, which is supported by the National Science Foundation.

References

Barron, E.J., Hay, W.W., Thompson, S., 1989. The hydrologic cycle: a major variable during Earth history. Palaeogeogr., Palaeoclimatol., Palaeoecol. 75, 157–174.

Benson, L.V., 1981. Paleoclimatic significance of lake-level fluctuations in the Lahontan Basin. Quat. Res. 16, 390–403.

Berger, A., 1978. Long-term variations of daily insolation and Quaternary climatic changes. J. Atmos. Sci. 35, 2362–2367.

Bradley, W.H., 1963. Paleolimnology. In: Frey, D.G. (Ed.), Limnology in North America. University of Wisconsin Press, Madison, pp. 621–652.

Bradley, W.H., 1973. Oil shale formed in desert environment: Green River Formation, Wyoming. Geol. Soc. Am. Bull. 84, 1121–1124.

Bradley, W.H., Eugster, H.P., 1964. Geochemistry and paleolimnology of the trona deposits and associated authigenic minerals of the Green River Formation of Wyoming. U.S. Geological Survey Professional Paper 496-B, 71 pp.

Carroll, A.R., Bohacs, K.M., 1999. Stratigraphic classification of ancient lakes: balancing tectonic and climatic controls. Geology 27, 99–102.

Cerda, A., 1996. Seasonal variability of infiltration rates under contrasting slope conditions in southeast Spain. Geoderma 69, 217–232.

Cerling, T.E., 1991. Carbon dioxide in the atmosphere: evidence from Cenozoic and Mesozoic paleosols. Am. J. Sci. 291, 377–400.

Dettman, D.L., Lohmann, K.C., 2000. Oxygen isotope evidence for high-altitude snow in the Laramide Rocky Mountains of North America during the late Cretaceous and Paleogene. Geology 28, 243–246.

Dickinson, D.R., Yepsen, J.H., Hales, J.V., 1965. Saturated vapor pressures over Great Salt Lake brines. J. Geophys. Res. 70, 500–503.

Dickinson, W.R., Klute, M.A., Hayes, M.J., Janecke, S.U., Lundin, E.R., McKittrick, M.A., Olivares, M.D., 1988. Paleogeographic and paleotectonic setting of Laramide sedimentary basins in the central Rocky Mountain region. Geol. Soc. Am. Bull. 100, 1023–1039.

Dickinson, R.E., Henderson-Sellers, A., Kennedy, P.J., 1993. Biosphere–atmosphere transfer scheme (BATS) version 1e as coupled to the NCAR community climate model. NCAR Technical Note NCAR/TN-387+STR. National Center for Atmospheric Research, Boulder, Colorado, 72 pp.

Eugster, H.P., 1971. Origin and deposition of trona. Contrib. Geol. 10, 49–56, University of Wyoming.

Eugster, H.P., Hardie, L.A., 1975. Sedimentation in an ancient playa-lake complex: The Wilkins Peak Member of the Green River Formation of Wyoming. Geol. Soc. Am. Bull. 86, 319–334.

Fischer, A.G., Roberts, L.T., 1991. Cyclicity in the Green River Formation (Lacustrine Eocene) of Wyoming. J. Sediment. Petrol. 61, 1146–1154.

Freeman, K.H., Hayes, J.M., 1992. Fractionation of carbon isotopes by phytoplankton and estimates of ancient CO_2 levels. Global Biogeochem. Cycles 6, 185–198.

Fritz, W.J., Harrison, S., 1985. Early Tertiary volcaniclastic deposits of the northern Rocky Mountains. In: Flores, R.M., Kaplan, S.S. (Eds.), Cenozoic Paleogeography of the West-Central United States. Society of Economic Paleontologists and Mineralogists, Denver, pp. 383–402.

Gill, A.E., 1982. Atmosphere–Ocean Dynamics. Academic Press, New York, 662 pp.

Glenn, C.R., Kelts, K., 1991. Sedimentary rhythms in lake deposits. In: Einsele, G., Ricken, W., Seilacher, A. (Eds.), Cycles and Events in Stratigraphy. Springer, Berlin, pp. 188–221.

Herbert, T.D., Fischer, A.G., 1986. Milankovitch climatic origin of mid-Cretaceous black shale rhythms in central Italy. Nature 321, 739–743.

Hostetler, S.W., Bartlein, P.J., 1990. Simulation of lake evaporation with application to modeling lake level variations of Harney-Malheur Lake, Oregon. Water Resour. Res. 26, 2063–2612.

Krishtalka, L., West, R.M., Black, C.C., Dawson, M.R., Flynn, J.J., Turnbull, W.D., Stucky, R.K., McKenna, M.C., Bown, T.M., Golz, D.J., Lillegraven, J.A., 1987. Eocene (Wasatchian through Duchesnean) biochronology of North America. In: Woodhouse, M.O. (Ed.), Cenozoic Mammals of North America. University of California Press, Berkeley, pp. 77–117.

Kutzbach, J.E., 1980. Estimates of past climate at paleolake Chad, North Africa, based on a hydrologic and energy-balance model. Quat. Res. 14, 210–223.

Kutzbach, J.E., Street-Perrott, F.A., 1985. Milankovitch forcing of fluctuations in the level of tropical lakes from 18 to 0 kyr BP. Nature 317, 130–134.

Leopold, E.B., MacGinitie, H.D., 1972. Development and affinities of Tertiary floras in the Rocky Mountains. In: Graham, A. (Ed.), Floristics and Paleofloristics of Asia and Eastern North America. Elsevier, New York, pp. 147–200.

MacGinitie, H.D., 1969. The Eocene Green River Flora of Northwestern Colorado and Northeastern Utah. University of California Press, Berkeley, 203 pp.

Manabe, S., Wetherald, R.T., 1975. The effects of doubling the CO_2 concentration on the climate of a general circulation model. J. Atmos. Sci. 32, 3–15.

Mason, I.M., Guzkowska, M.A.J., Rapley, C.G., 1994. The response of lake levels and areas to climatic change. Clim. Change 27, 161–197.

Matthews, M.D., Perlmutter, M.A., 1994. Global cyclostratigraphy: an application to the Eocene Green River Basin. Spec. Publ. Int. Assoc. Sedimentol. 19, 459–481.

Meyer, H.W., 1992. Lapse rates and other variables applied to estimating paleoaltitudes from fossil floras. Palaeogeogr., Palaeoclimatol., Palaeoecol. 99, 71–99.

Morrill, C., Koch, P.L., 1999. Isotopic data from freshwater bivalves of the Green River Formation (Eocene): implications for high elevation snow. Geol. Soc. Am. Abstr. Programs 31, A360.

Norris, R.D., Jones, L.S., Corfield, R.M., Cartlidge, J.E., 1996. Skiing in the Eocene Uinta Mountains? Isotopic evidence in the Green River Formation for snow melt and large mountains. Geology 24, 403–406.

Olsen, P.E., Kent, D.V., 1996. Milankovitch climate forcing in the tropics of Pangaea during the Late Triassic. Palaeogeogr., Palaeoclimatol., Palaeoecol. 122, 1–26.

Pollard, D., Schulz, M., 1994. A model for the potential locations of Triassic evaporite basins driven by paleoclimatic GCM simulations. Global Planet. Change 9, 233–249.

Pollard, D., Thompson, S.L., 1995. Use of a land-surface-transfer scheme (LSX) in a global climate model: the response to doubling stomatal resistance. Global Planet. Change 10, 129–161.

Pollard, D., Thompson, S.L., 1997. Climate and ice-sheet mass-balance at the last glacial maximum from the GENESIS version 2 global climate model. Quat. Sci. Rev. 16, 841–863.

Roehler, H.W., 1993. Eocene climates, depositional environments, and geography, greater Green River Basin, Wyoming, Utah, and Colorado. U.S. Geological Survey Professional Paper 1506-F, 74 pp.

Scotese, C.R., Golonka, J., 992. Paleogeographic Atlas: University of Texas, Arlington PALEOMAP Progr. Report 20.

Sellers, W.D., 1965. Physical Climatology. University of Chicago Press, 272 pp.

Short, D.A., Mengel, J.G., Crowley, T.J., Hyde, W.T., North, G.R., 1991. Filtering of Milankovitch cycles by earth's geography. Quat. Res. 35, 157–173.

Sinha, A., Stott, L.D., 1994. New atmospheric pCO_2 estimates from paleosols during the late Paleocene/early Eocene global warming interval. Global Planet. Change 9, 297–307.

Sloan, L.C., Rea, D.K., 1995. Atmospheric carbon dioxide and early Eocene climate: a general circulation modeling sensitivity study. Palaeogeogr., Palaeoclimatol., Palaeoecol. 119, 275–292.

Small, E.E., Sloan, L.C., Hostetler, S.W., Giorgi, F., 1999. Simulating the water balance of the Aral Sea with a coupled modeling system. J. Geophys. Res. 104, 6583–6602.

Smoot, J.P., 1983. Depositional subenvironments in an arid closed basin: the Wilkins Peak Member of the Green River Formation (Eocene), Wyoming, USA. Sedimentology 30, 801–827.

Sorrisovalvo, M., Bryan, R.B., Yair, A., Iovino, F., Antronico, L., 1995. Impact of afforestation on hydrological response and sediment production in a small Calabrian catchment. Catena 25, 89–104.

Surdam, R.C., Stanley, K.O., 1980. Effects of changes in drainage-basin boundaries on sedimentation in Eocene Lakes Gosiute and Uinta of Wyoming, Utah, and Colorado. Geology 8, 135–139.

Thompson, S.L., Pollard, D., 1995. A global climate model (GENESIS) with a land-surface transfer scheme (LSX): Part I. Present climate simulation. J. Clim. 8, 732–761.

Thompson, S.L., Pollard, D., 1997. Greenland and Antarctic mass balances for present and doubled atmospheric CO_2 from the GENESIS version 2 global climate model. J. Clim. 10, 871–900.

Weedon, G.P, Jenkyns, H.C., 1990. Regular and irregular climatic cycles and the Belemnite Marls (Pliensbachian, Lower Jurassic, Wessex Basin). J. Geol. Soc. (London) 147, 915–918.

Wilf, P., 2000. Late Paleocene–early Eocene climate changes in southwestern Wyoming: Paleobotanical analysis. Geol. Soc. Am. Bull. 112, 292–307.

Wilf, P., Wing, S.L., Greenwood, D.R., Greenwood, C.L., 1998. Using fossil leaves as paleoprecipitation indicators: an Eocene example. Geology 26, 203–206.

Zachos, J.C., Stott, L.D., Lohmann, K.C., 1994. Evolution of early Cenozoic marine temperatures. Paleoceanography 9, 353–387.